

Theory of Polymer Diffusion in Polymer-Nanoparticle Mixtures: Effect of Nanoparticle Loading and Polymer Chain Length

Bokai Zhang,^{1,*} Jian Li,² Juan-mei Hu,¹ and Lei Liu^{1,†}

¹*Department of Physics, Zhejiang Sci-Tech University, Hangzhou 310018, China*

²*Department of Physics and Electronic Engineering, Heze University, Heze 274015, China*

The theoretical description for dynamics of polymer-nanoparticle (NP) mixtures has been a tough challenge due to their multiple system-specific factors. In this letter, a microscopic theoretical framework for polymer diffusion in the mixtures is constructed. The parameter-free theory has an explicit expression and remains tractable on pair correlation level with system-specific equilibrium structures as input. In a minimal polymer-NP mixture model, our theory correctly captures the effect of NP loading and polymer chain length. The prediction for the NP-induced reduction of the diffusion shows reasonable agreement with recent simulations. Subsequently, the curve of diffusion versus chain length exhibits a power-law decay at dense NPs and/or long chain. The scaling exponent is proposed to characterize chain motion in complex environments. We expect precise measurements for the scaling exponent in future experiment and simulation. The work provides a first-principle theoretical foundation to investigate dynamic problems in diverse polymer nanocomposites.

Understanding the diffusion of flexible polymer in polymer-nanoparticle (NP) mixtures is an important problem being widely related to transport of biopolymer [1–3], drug delivery [4, 5] and the properties and processability of polymer nanocomposites (PNCs) materials [6, 7]. The description of dynamics in polymer-NP mixtures involves multiple system-specific factors, including the characteristics of NP (e.g., sizes, shapes, interface softness, and concentration) and polymer (e.g., topology, molecular weight, and rigidity) and polymer-NP interaction. Yet, a theory for polymer diffusion on these factors represents a tough challenge and poses a complex problem, where the motion of polymer and NP is interrelated, thus significantly influencing each other.

In the polymer-NP mixtures, NP diameter, volume fraction and polymer chain length are basic variables to control structure and dynamics. Their effect on various properties of the mixtures has attracted an enormous amount of research using computer simulations and experimental approaches as well as some phenomenological models [8–19]. Experiments of polymer tracer in athermal NPs using elastic recoil detection (ERD) reveal remarkable reduction of the polymer diffusion compared to their motion in the bulk [12, 13]. Recently, a universal relation between polymer diffusion and the average interparticle distance normalized by the radius of gyration h/R_g has been reported, suggesting that h/R_g captures the effect of NP size, size polydispersity, and volume fraction on polymer dynamics. In addition, by measuring single chain dynamic structure factor in PNCs, Schneider *et al.* found that NP loading can lead to a crossover from chain entanglement to NP entanglement, for which chain diffuses in a tube formed by NPs rather than surrounding chains [17]. In the aspect of size ratio of chain length to NP diameter, molecular simulation and Nonlinear Langevin equation theory reveal that small NPs induce more pronounced reduction in polymer diffusion, greater variation in glass transition tempera-

ture and higher dynamic fragility [18, 19]. In theoretical model, polymer diffusion in the network of PNCs is mapped to the motion of spheres through hollow cylinders [16]. An analytical expression for the polymer diffusion is obtained. But the approach is oversimplified and neglects detailed information, e.g., chain conformation and microscopic interaction.

In this letter, we aim to develop a microscopic and parameter-free theory linking equilibrium structure with the long-time center-of-mass (CM) diffusion of polymer. An explicit expression for the diffusion coefficient is derived in the framework of naive mode-coupling theory (naive-MCT[20]) which has been successfully applied to NP diffusion in PNCs [21], activated dynamics in binary mixtures [22, 23] and cross-linked networks [24]. In a minimal polymer-NP mixture model, the microscopic theory is used to incorporate the effect of NP loading and polymer chain length.

We consider a binary mixture of hard spheres (diameter σ_n) and nonadsorbing flexible polymers (radius of gyration R_g). The polymer chain is modeled as a Gaussian thread chain consisting of N_p segments of diameter l_p [25]. The limit of dilute polymer is taken, that is, the interactions between polymers are neglected. We adopt $\sigma_n/l_p = 10$, given that the NP diameter σ_n is much greater than segment diameter l_p . In this model, the structure and dynamics of the polymer-NP mixture are controlled by two key variables: NP volume fraction, ϕ_n , and polymer-NP size ratio, R_g/σ_n . The units of length and energy are respectively $[L] = \sigma_n$ and $[E] = k_B T$.

Here we sketch the key physical ideas and main theoretical results. The technical details are given in the Supporting Information. First, we formulate the long-time resistance of tagged chain on the CM level based on Mori-Zwanzig projection operator technique and MCT approximation [26, 27], which can incorporate frictional effect arising from surrounding environment. The resistance captures NP-induced friction and single chain con-

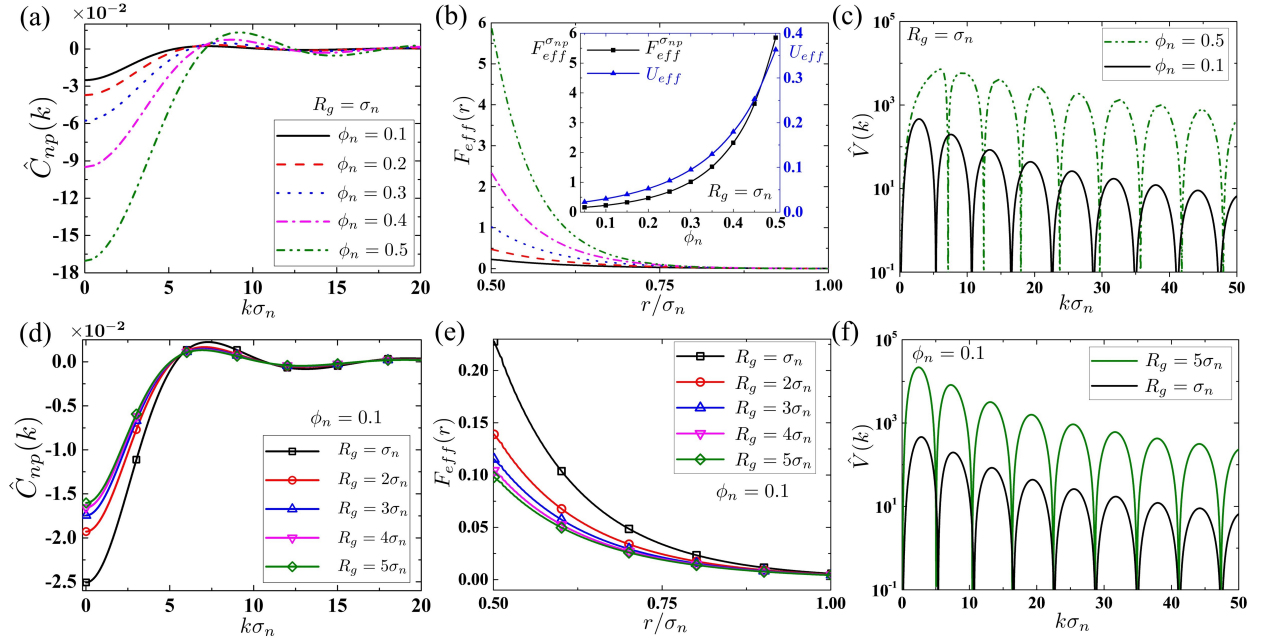


FIG. 1. (a) Plots of DCF versus wavevector for several NP volume fractions at $R_g = \sigma_n$. (b) segment-NP distance dependence of effective force. The legend is the same as in (a). Inset: The contact value of effective force (black square line) and effective frictional work (blue triangle line) versus NP volume fraction. (c) Static part of force-force vertex function for two NP volume fractions, $\phi_n = 0.1$ and $\phi_n = 0.5$. (d) Plots of DCF versus wavevector for several chain lengths at $\phi_n = 0.1$. (e) NP-segment distance dependence of effective force for several chain lengths. (f) Static part of force-force vertex function for two chain lengths $R_g = 5\sigma_n$ and $R_g = \sigma_n$.

formation. Starting from the generalized Langevin equation for the CM of polymer [28], the memory kernel is related to force-force correlation function by $K_{CM}(t) = \frac{1}{3k_B T} \langle \mathbf{F}_{CM}(0) \cdot \mathbf{F}_{CM}(t) \rangle$, where the total force exerted on a polymer is $\mathbf{F}_{CM} = \sum_i^{N_p} \mathbf{F}_i$. The resistance is obtained by integrating the memory kernel over time, $\xi_{CM} = \int_0^\infty K_{CM}(t) dt$. In the framework of naive-MCT, standard closure projects the total force on a bilinear product of tagged chain density and collective density fluctuation. And then four-point correlation is approximately factorized into pair correlations. Finally, the long-time resistance is expressed as

$$\xi_{CM} = \frac{\rho_n k_B T}{6\pi^2} \int_0^\infty dk \int_0^\infty dt \hat{V}(k) \hat{\Gamma}_{nn}^c(k, t) \hat{\Gamma}_p^s(k, t), \quad (1)$$

where the static part of force-force vertex function $\hat{V}(k)$ represents time independent contribution to the resistance involving different length scales, including chain length N_p , direct correlation function (DCF) between NP and segment $\hat{C}_{np}(k)$, static structure factor for NPs $\hat{S}_{nn}(k)$ and intramolecular structure factor $\hat{\omega}_p(k)$,

$$\hat{V}(k) = N_p k^4 \hat{\omega}_p(k) \hat{C}_{np}^2(k) \hat{S}_{nn}(k). \quad (2)$$

The time dependent part is the force relaxation channel via density correlation propagator of tagged polymer, $\hat{\Gamma}_p^s = \langle \exp(i\mathbf{k} \cdot (\mathbf{R}_s(t) - \mathbf{R}_s(0))) \rangle$ and collective density correlation propagator of NPs, $\hat{\Gamma}_{nn}^c =$

$\sum_{i,j}^{N_n} \langle \exp(i\mathbf{k} \cdot (\mathbf{R}_i(t) - \mathbf{R}_j(0))) \rangle$. Some simple expressions for these propagators are adopted to make our theory analytically tractable (see Supporting Information).

Further, the long-time diffusion coefficient is related to the resistance by the well-known Einstein relation, $D_p = k_B T / \xi_p$. We assume the total resistance ξ_p contains two parts, $\xi_p = \xi_{bulk} + \xi_{CM}$. ξ_{bulk} is the resistance for single chain in the bulk without adding NPs and can be obtained based on the Rouse model [29], $\xi_{bulk} = 6\pi l_p N_p \eta_0$. Final expression for the polymer diffusion coefficient normalized by its value in the bulk, $D_{p0} = k_B T / \xi_{bulk}$, is explicitly derived as

$$D_r = \frac{D_p}{D_{p0}} = \frac{1}{1 + \frac{\rho_n}{6\pi^2} \int_0^\infty dk k^2 \hat{\omega}_p^2 \hat{C}_{np}^2 \hat{S}_{nn}}. \quad (3)$$

These equilibrium structure functions depend on NP volume fraction, polymer chain length and interactions in the mixtures. Here, we adopt the polymer reference interaction site model (PRISM) approach with thermodynamic consistency consideration and an extra modified Percus-Yevick (PY) closure to calculate them [25]. In the approach, the modified PY closure captures chain connectivity, that is, the change of chain conformation as segments are close to NPs. Complete expressions can be found in Supporting Information.

We first focus on NP loading effect on equilibrium structure and effective interaction. As shown in Figure

1a, wavevector-dependent DCF is strongly dependent on NP volume fraction. Quantitatively, when ϕ_n increases from 0.1 to 0.5, the magnitude of DCF at $k \rightarrow 0$ increases nearly seven times, from $|\hat{C}_{np}(k \rightarrow 0)| \approx 0.025$ to $|\hat{C}_{np}(k \rightarrow 0)| \approx 0.170$. The behavior of $\hat{C}(k)$ around zero wavevector is considered to determine large-scale physical properties, such as thermodynamics and phase boundary in polymer melts and PNCs [30, 31]. Moreover, there is a significant increase in the height of primary peak in \hat{C}_{np} with increase of ϕ_n , corresponding to more compact local packing between NPs and segments. The peak position, q_{max} , is closely related to the mean intermolecular distance, which is estimated as $r_{mean} \sim 2\pi/q_{max}$. Figure 1a shows that the peak position q_{max} has a shift with adding NPs, from $q_{max} \approx 7.6 \sim 9.2\sigma_n^{-1}$, that is, $r_{mean} \approx 0.83 \sim 0.68\sigma_n$.

In real space, real force exerted by surrounding particles can be renormalized as effective force between NP and segment, which is defined as $\mathbf{F}_{eff}^{np}(r) = -k_B T \nabla C_{np}(r)$. As illustrated in Figure 1b, the positive value of effective force indicates repulsive interaction between hard NP and nonadsorbing segment. The magnitude of the effective force exhibits a significant increase with NPs volume fraction ϕ_n . Specifically, the contact value of effective force at $\sigma_{np} = (\sigma_n + \sigma_p)/2$ increases from $F_{eff}^{np}(\sigma_{np}) \approx 0.16$ to 5.85 with $\phi_n = 0.05 \sim 0.5$ which is plotted in the inset of Figure 1b.

To further quantify frictional effect arising from NPs, a renormalized effective frictional work (EFW) is introduced as $U_{eff} = \int_{\sigma_{np}}^{\infty} \mathbf{F}_{eff}(\mathbf{r}) \cdot d\mathbf{r}$. Physically, U_{eff} equals to the work of effective force driving the NP-segment distance from σ_{np} to infinity. Due to the definition of effective force, the EFW exactly equals to negative contact value of DCF in real space except an energy unit $k_B T$, $U_{eff} = -k_B T C_{np}(\sigma_{np})$. As shown in the inset of Figure 1b, adding NPs strongly enhances the EFW, $U_{eff} \approx 0.023$ to $U_{eff} \approx 0.363$ with $\phi_n = 0.05 \sim 0.5$. Besides we also find that the loading of NPs leads to a significant increase in the amplitude and enveloping area of the vertex function (see Figure 1c).

In dynamics, as seen in experiments and simulations [13, 18], the normalized diffusion coefficient rapidly decays with loading of NPs as shown in Figure 2a. Moreover, the diffusion exhibits a more drastic decrease for longer chain. For instance, D_p decays to 20% of D_{p0} at $\phi_n \approx 0.12$ for $R_g = 3.14\sigma_n$, whereas it decays to the same value at $\phi_n \approx 0.41$ for $R_g = 1.26\sigma_n$. Our theoretical prediction for the polymer chain length dependence of D_r - ϕ_n curve is qualitatively in agreement with simulation for Lennard-Jones particles as shown in the symbols of Figure 2a. At a small amount of NP loadings, theoretical results for polymer diffusion are quantitatively consistent with the simulation data.

In simulation for polymer-NP mixtures [18], an empirical function describing the relation between D_r and ϕ_n

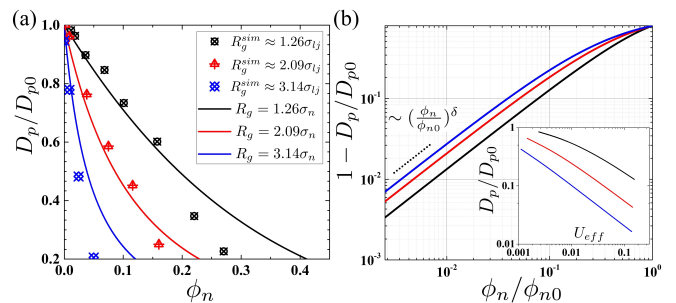


FIG. 2. (a) Normalized polymer diffusion, D_p/D_{p0} versus ϕ_n for several chain lengths computed from our theory (solid lines). Simulation results are also plotted (symbols, ref 18), where the radius of gyration changes less than 8% and thus is assumed as constant here. (b) Plots of $1 - D_p/D_{p0}$ versus ϕ_n rescaled by the cutoff volume fraction ϕ_{n0} , where $D_p(\phi_{n0})/D_{p0} = 0.2$. The legend is the same as in (a). The dotted line represents power-law behavior described by eq 4. Inset: Normalized polymer diffusion versus effective frictional work.

is proposed

$$D_r = 1 - (\phi_n/\phi_{n0})^\delta. \quad (4)$$

The cutoff volume fraction ϕ_{n0} represents arrest of motion of polymers, which is empirically defined by $D_r(\phi_{n0}) = 0.2$. Figure 2b shows our theoretical predictions for $1 - D_r$ as a function of NP volume fraction rescaled by ϕ_{n0} . We find that eq 4 does a good description for normalized diffusion at a small amount of NPs loading and the scaling exponent δ is approximately equal to 1 for all radii of gyration we studied. For high volume fraction, namely, $\phi_n/\phi_{n0} > 0.1$, the polymer diffusion deviates from the description of eq 4. In the inset of Figure 2b, the polymer diffusion exhibits a significant decrease with EFW, suggesting that the loading of NPs enhances effective frictional interaction and thus suppresses the motion of polymer chain.

An average interparticle distance (ID) is introduced to quantify the NP-induced confinement effect. The ID is calculated by $h(\phi_n) = \sigma_n[(\phi_{RCP}/\phi_n)^{1/3} - 1]$, where the random closed packing is taken as $\phi_{RCP} = 0.64$. Here, we focus on the dependence of the normalized polymer diffusion on the ID normalized by the radius of gyration, $h/2R_g$. We calculate $D_r(h/2R_g)$ by changing ϕ_n at fixed R_g (red line in Figure 3) and by changing R_g at fixed ϕ_n (blue line in Figure 3). In general, D_r drastically decreases as the $h/2R_g$ falls to zero and recovers to 1 for large normalized ID. The dashed-dotted line in Figure 3 indicates a universal curve found in molecular dynamics simulation [18], which shows similar behavior to our theoretical predictions. It can be described by an empirical expression,

$$D_r = 1 - \exp\left(-\frac{\alpha h}{2R_g}\right). \quad (5)$$

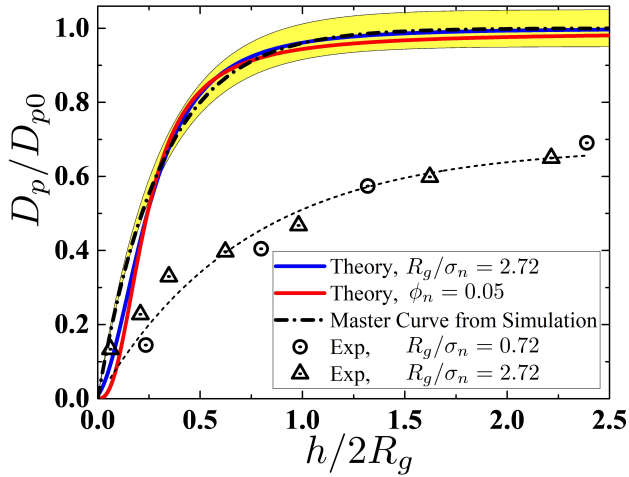


FIG. 3. Normalized polymer diffusion versus ID normalized by the radius of gyration at fixed size ratio of chain length to NP diameter $R_g/\sigma_n = 2.72$ (blue line) and fixed $\phi_n = 0.05$ (red line), respectively. The experimental results for two polymer-NP size ratios (symbols, ref 13) and a universal curve obtained from simulation (dashed-dotted line, ref 18) are plotted. The yellow shaded area represents $y = 1 - \exp(-3.3x)$ with 5% error. The dashed line is guided to the eye.

The yellow shaded area in Figure 3 shows the D_r - h curve predicted by eq 5 at $\alpha = 3.3$ with relative error 5%. Further, ERD experiment has reported the data between D_r and $h/2R_g$ can also collapse to a universal curve but is different from theoretical and simulation results (see the symbols of Figure 3). Based on current general perception, despite some universal relations are reported [12, 13, 18], polymer dynamics depend strongly on the details in various polymer nanocomposite materials [15, 32, 33]. In our theory, some effects of these system-specific factors can be included into equilibrium structure and thus influence polymer diffusion through eq 3.

We turn to focus on chain length effect on structure and dynamics. As shown in Figure 1d, the DCF exhibits a milder decrease in magnitude with the radius of gyration in comparison to NP volume fraction. The fall of $|\hat{C}(k \rightarrow 0)|$ is less than 40% when the size ratio increases from $R_g/\sigma_n = 1$ to $R_g/\sigma_n = 5$. Our calculation also shows that the increase of chain length leads to a decrease of effective force at fixed NP volume fraction (see Figure 1e). The varying trend is consistent with that of DCF.

The wavevector-dependent static vertex functions for two different size ratios, $R_g/\sigma_n = 1$ and $R_g/\sigma_n = 5$, are shown in Figure 1f. The peak position keeps almost unchanged for all studied chain lengths. It implies that chain length cannot change average distance between NP and segment. The amplitude and enveloping area of vertex function increases with chain length. We notice that chain length dismisses liquid structure on the segment

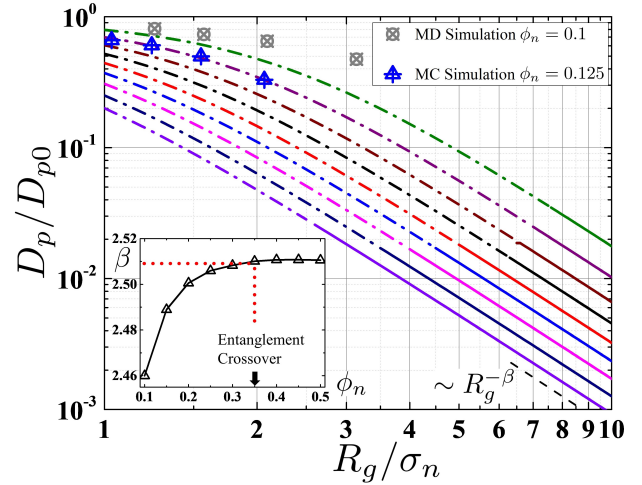


FIG. 4. Normalized polymer diffusion versus the size ratio of the radius of gyration to NP diameter with several NP volume fractions, from $\phi_n = 0.1$ (top) to $\phi_n = 0.5$ (bottom). The solid lines represent the regime of power-law behavior, $D_p/D_{p0} \sim R_g^{-\beta}$. Data from molecular dynamics simulation (ref 18) and Monte Carlo simulation (ref 34) is plotted, respectively (symbols). Inset: The scaling exponent for several ϕ_n . The dotted red lines mark the value of scaling exponent at entanglement crossover NP volume fraction predicted by experiment (ref 17), $\beta(\phi_{nc} = 0.35) \approx 2.51$.

scale, such as DCF and effective force (see Figure 1d and 1e). But on the polymer CM level, chain length has a remarkable contribution through N_p and $\hat{\omega}_p$ into the vertex function and then into the resistance through the integral kernel in eq 3.

Furthermore, we investigate the normalized polymer diffusion as a function of the polymer-NP size ratio R_g/σ_n for different NP volume fractions. The normalized diffusion coefficient monotonically decreases with the size ratio. The NP-induced reduction of diffusion of long chain is more remarkable than that of short chain as shown in Figure 4. More prominently, in long chain and/or high NP loading, the polymer diffusion exhibits a power-law decay, $D_r \sim R_g^{-\beta}$, as illustrated in the solid lines of Figure 4. The power-law regime arises at smaller R_g/σ_n for higher ϕ_n . The scaling exponent is predicted as $\beta \approx 2.46$ at $\phi_n = 0.1$, and tends to $\beta \approx 2.51$ at $\phi_n > 0.35$. In polymer physics, the relation between polymer diffusion and segment number is scaled as $D_p \sim N_p^{-X}$, where the diffusion scaling exponent X depends on different surrounding environments [35]. Combining the radius of gyration $R_g^2 = N_p l_p^2 / 6$ for Gaussian chain and $D_{p0} \sim N_p^{-1}$ for Rouse model, the relation of scaling exponents between X and β is obtained as $X = \beta/2 + 1$. Therefore, the prediction of our microscopic theory for the diffusion scaling exponent is obtained as $X_{mix} = 2.230 \sim 2.225$.

In the phenomenological Doi-Edwards reptation theory for entangled polymer melts, single chain is consid-

ered to be confined in an existing virtual tube formed by surrounding polymers [29]. The chain cannot move transversely across this tube due to the spatial confinement. The diffusion and relaxation of polymers are via reptation motion of two ends of chain under frictional force f_{tube} . The frictional force scales with the polymer segment number as $f_{tube} \sim N_p^\gamma$. The duration moving out of the existing tube is proportional to the frictional force, $\tau_{tube} \sim f_{tube}L^2$, where L is chain length and thus $L \sim N_p$. The relation between polymer diffusion and segment number is obtained by $D_p \sim R_g^2/\tau_{tube} \sim N_p^{-1-\gamma}$. The Doi-Edwards theory predicts the exponent $\gamma = 1$ and thus $X_{melt} = 2$. In the polymer-NP mixtures, our calculation for the scaling exponent X_{mix} corresponds to $\gamma \approx 1.230 \sim 1.225$. Essentially, the scaling exponent γ reflects the frictional effect arising from fluctuating force in an existing tube formed by surrounding polymers or NPs. We believe that the exponent can characterize chain motion in various complicated environments.

In small-angle neutron scattering experiment, there are two types of entanglement in the polymer-NP mixtures, chain entanglement and NP entanglement dominating at low and high NP loading, respectively [17]. A crossover NP volume fraction $\phi_{nc} = 0.35$ is found where the two types of entanglement have an identical contribution. Our theory predicts the scaling exponent $X_{mix,c} = \beta/2 + 1 \approx 2.25$ at $\phi_{nc} = 0.35$ and remains almost constant at higher ϕ_n as shown in the inset of Figure 4. In coarse-grained molecular simulations, qualitative decrease of normalized diffusion coefficient with the size ratio R_g/σ_n is indeed observed (see symbols in Figure 4) [18, 34]. However, the exact value of β cannot be determined due to lack of enough data in the situation of long chain or dense NPs. The more precise measurement for the scaling exponent is expected in future simulation and experiment.

In conclusion, we have constructed a first-principle theory for polymer diffusion in polymer-NP mixtures. The explicit expression for the normalized polymer diffusion is derived with the system-specific equilibrium structures as input. Our theory predicts the effect of NP volume fraction and polymer chain length in a minimal polymer-NP mixture model. More broadly, our tractable theory provides a foundation for various open problems about polymer dynamics, such as (i) attractive NP-polymer interaction, (ii) polymer with rigidity or more complicated internal structure, such as single-chain NPs and ring polymers [36, 37]. Theoretical work is ongoing in all these directions.

This work is supported by National Natural Science Foundation of China (No.11904320, No.11847115, and No.11804085), Natural Science Foundation of Zhejiang Province (No.LQ18B040002) and the Fundamental Research Funds of Zhejiang Sci-Tech University (No.18062243-Y).

* bkzhang@zstu.edu.cn

† leiliu@zstu.edu.cn

- [1] S. K. Lai, D. E. O'Hanlon, S. Harrold, S. T. Man, Y.-Y. Wang, R. Cone, and J. Hanes, *Proc. Natl. Acad. Sci. USA*, **104**, 1482 (2007).
- [2] K. A. Woodrow, Y. Cu, C. J. Booth, J. K. Saucier-Sawyer, M. J. Wood, and W. M. Saltzman, *Nat. Mater.* **8**, 526–533 (2009).
- [3] H.-X. Zhou, G. Rivas, and A. P. Minton, *Annu. Rev. Biophys.* **37**, 375 (2008).
- [4] I. Brigger, C. Dubernet, and P. Couvreur, *Adv. Drug Deliv.* **64**, 24 (2012).
- [5] D. A. LaVan, T. McGuire, and R. Langer, *Nat. Biotechnol.* **21**, 1184–1191 (2003).
- [6] S. K. Kumar, B. C. Benicewicz, R. A. Vaia, and K. I. Winey, *Macromolecules* **50**, 714 (2017).
- [7] S. K. Kumar, V. Ganesan, and R. A. Riggleman, *J. Chem. Phys.* **147**, 020901 (2017).
- [8] E. J. Bailey and K. I. Winey, *Prog. Polym. Sci.* **105**, 101242 (2020).
- [9] S. Gong, Q. Chen, J. F. Moll, S. K. Kumar, and R. H. Colby, *ACS Macro Lett.* **3**, 773 (2014).
- [10] A. P. Holt, J. R. Sangoro, Y. Wang, A. L. Agapov, and A. P. Sokolov, *Macromolecules* **46**, 4168 (2013).
- [11] M. Krutyeva, A. Wischniewski, M. Monkenbusch, L. Willner, J. Maiz, C. Mijangos, A. Arbe, J. Colmenero, A. Radulescu, O. Holderer, M. Ohl, and D. Richter, *Phys. Rev. Lett.* **110**, 108303 (2013).
- [12] J. Choi, M. J. A. Hore, J. S. Meth, N. Clarke, K. I. Winey, and R. J. Composto, *ACS Macro Lett.* **2**, 485 (2013).
- [13] S. Gam, J. S. Meth, S. G. Zane, C. Chi, B. A. Wood, M. E. Seitz, K. I. Winey, N. Clarke, and R. J. Composto, *Macromolecules* **44**, 3494 (2011).
- [14] C. Echeverria and R. Kapral, *J. Chem. Phys.* **132**, 104902 (2010).
- [15] A. Karatrantos, R. J. Composto, K. I. Winey, and N. Clarke, *J. Chem. Phys.* **146**, 203331 (2017).
- [16] J. S. Meth, S. Gam, J. Choi, C.-C. Lin, R. J. Composto, and K. I. Winey, *J. Phys. Chem. B* **117**, 15675 (2013).
- [17] G. J. Schneider, K. Nusser, L. Willner, P. Falus, and D. Richter, *Macromolecules* **44**, 5857 (2011).
- [18] V. Sorichetti, V. Hugouvieux, and W. Kob, *Macromolecules* **51**, 5375 (2018).
- [19] S. Cheng, S.-J. Xie, J.-M. Y. Carrillo, B. Carroll, H. Martin, P.-F. Cao, M. D. Dadmun, B. G. Sumpter, V. N. Novikov, K. S. Schweizer, and A. P. Sokolov, *ACS Nano* **11**, 752 (2017).
- [20] T. R. Kirkpatrick and P. G. Wolynes, *Phys. Rev. A* **35**, 3072 (1987).
- [21] U. Yamamoto and K. S. Schweizer, *J. Chem. Phys.* **135**, 224902 (2011).
- [22] R. Jadrich and K. S. Schweizer, *Phys. Rev. E* **86**, 061503 (2012).
- [23] R. Zhang and K. S. Schweizer, *J. Phys. Chem. B* **122**, 3465 (2018).
- [24] Z. E. Dell and K. S. Schweizer, *Macromolecules* **47**, 405 (2014).
- [25] M. Fuchs and K. S. Schweizer, *Phys. Rev. E* **64**, 021514 (2001).
- [26] R. Zwanzig, *Nonequilibrium Statistical Mechanics* (Oxford University Press, 2001).

- [27] W. Götze, *Complex Dynamics of Glass-Forming Liquids: A Mode-Coupling Theory* (Oxford University Press, 2008).
- [28] J.-P. Hansen and I. R. McDonald, *Theory of Simple Liquids* (Academic Press, 2013).
- [29] M. Doi and S. F. Edwards, *The Theory of Polymer Dynamics*, Vol. 73 (Oxford University Press, 1988).
- [30] K. Chen and K. S. Schweizer, *J. Chem. Phys.* **126**, 014904 (2007).
- [31] L. M. Hall and K. S. Schweizer, *J. Chem. Phys.* **128**, 234901 (2008).
- [32] T. Desai, P. Koblinski, and S. K. Kumar, *J. Chem. Phys.* **122**, 134910 (2005).
- [33] W.-S. Tung, P. J. Griffin, J. S. Meth, N. Clarke, R. J. Composto, and K. I. Winey, *ACS Macro Lett.* **5**, 735 (2016).
- [34] H. Zhang, D.-D. Sun, Y. Peng, J.-H. Huang, and M.-B. Luo, *Phys. Chem. Chem. Phys.* **21**, 23209 (2019).
- [35] T. C. B. McLeish, *Adv. Phys.* **51**, 1379 (2002).
- [36] E. Verde-Sesto, A. Arbe, A. J. Moreno, D. Cangialosi, A. Alegría, J. Colmenero, and J. A. Pomposo, *Mater. Horiz.* **7**, 2292 (2020).
- [37] Z. E. Dell and K. S. Schweizer, *Soft Matter* **14**, 9132 (2018).